# Optimal Cognitive Beamforming for Target Tracking in MIMO Radar/Sonar

Nathan Sharaga, Joseph Tabrikian, *Senior Member, IEEE*, and Hagit Messer, *Fellow, IEEE*

***Abstract*—In this paper, a cognitive beamforming method for target tracking by multiple-input multiple-output (MIMO) radar or sonar is proposed. In this method, at each step, the transmit beampattern is sequentially determined based on history observations. The conditional Bayesian Cramér-Rao bound (BCRB) for one-step prediction of the state-vector in target tracking problem was used as the optimization criterion for beampattern design. The proposed method is applied to the problem of target tracking in a shallow underwater environment in the presence of environmental uncertainties. It is shown that the method is able to automatically focus the transmit beampattern toward the target direction within a few steps at very low signal-to-noise ratios (SNRs). The method exhibits much better performance in terms of localization estimation error compared to other methods, such as orthogonal (omnidirectional) transmission.**

***Index Terms*—Cognitive beamforming, cognitive radar, sequential beamforming, sequential waveform design, target tracking, underwater acoustics.**

## I. Introduction

OPTIMAL beamforming for active arrays has been extensively studied in the past three decades. The optimization is usually performed in order to achieve better performance for detection or localization under some constraints, such as transmit power constraint. The optimization criterion may be lower bounds for localization performance, probability of detection, output signal-to-noise ratio (SNR), or information theoretic criteria.

Multiple-input multiple-output (MIMO) radar is an emerging technology that attracts the attention of researchers and practitioners alike [1]–[8]. In [1], [2] the colocated MIMO radar was introduced, in which it was shown that transmitting spatially orthogonal signals provides higher performance in estimation accuracy over traditional spatially coherent signals transmission. Several works have been devoted to transmit beamform design in MIMO radar systems [9]–[16]. In [9] it was shown that for a system with a small number of elements and low SNR, the MIMO radar system provides significant performance improvement over a monostatic phased array radar with high range and azimuth resolutions. In [10] a non-adaptive optimal beamform design for minimization of the Cramér-Rao bound (CRB) for target direction-of-arrival (DOA) and range estimation was studied. In [11], [12] the transmit signal waveform matrix is designed to satisfy constraints such as constant-modulus or low peak-to-average-power ratio constraints, given a pre-specified transmit autocorrelation matrix. In [13] the transmit autocorrelation matrix is adaptively designed to achieve a desired transmit beampattern. In [14] waveform design for clutter rejection has been studied. In [15] a non-adaptive optimal beamform design for a general MIMO detection problem, based on the Kullback-Leibler divergence between the densities of the observations under target presence and absence hypotheses, was studied.

A cognitive approach of transmit beamforming in radar systems was studied in [17]–[19], where the effectiveness of the adaptive transmit beamforming over non-adaptive transmit beamforming was demonstrated. A cognitive radar system adaptively interrogates the propagation channel using the available information from previous observations. This implies that the transmit waveforms can be sequentially adapted based on the information collected in the previous observations about the environment and the targets. In [17] a new cognitive beamforming approach was proposed for target parameters estimation by MIMO radar, where the beampattern in each pulse is adaptively determined based on previous observations. The algorithm was implemented in the case of free-space environment and non-dynamic target. This approach suggests a transmit beamforming design scheme, which adaptively minimizes the Bayesian CRB (BCRB) or the Reuven-Messer bound (RMB) [20] for estimating the system parameters based on historical observations. In [19] the problem of sequential transmit waveform design for target enumeration in cognitive radar is investigated. In the proposed technique, the transmit spatial waveform is adaptively determined at each step based on observations in the previous steps. The waveform is determined to minimize an approximated lower bound on the average sample number required to achieve given decision error rates.

Adaptive waveform design for moving target localization and tracking has been studied in several papers (see e.g. [21]–[27]). An adaptive approach of polarized waveform design method for target tracking under a framework of sequential Bayesian inference, was studied in [21]. In this approach, various parameters of the waveform were determined such that a BCRB based optimization criterion is satisfied. In [22] adaptive methods for target tracking and active sensing using waveform selection have been studied. The waveforms were determined to optimize tracking performance criteria, such

Manuscript received February 06, 2015; revised May 31, 2015; accepted July 25, 2015. Date of publication August 11, 2015; date of current version November 17, 2015. The guest editor coordinating the review of this manuscript and approving it for publication was Dr. Jean-Philippe Ovarlez.

N. Sharaga and H. Messer are with the School of Electrical Engineering, Tel-Aviv University, Tel-Aviv 39040, Israel (e-mail: natyshr@gmail.com; messer@eng.tau.ac.il).

J. Tabrikian is with the Department of Electrical and Computer Engineering, Ben-Gurion University of the Negev, Beer-Sheva 84105, Israel (e-mail: joseph@bgu.ac.il).

Color versions of one or more of the figures in this paper are available online at http://ieeexplore.ieee.org.

Digital Object Identifier 10.1109/JSTSP.2015.2467354

as minimizing the MSE of the target location estimation or maximizing target information retrieval. In [23] a waveform design algorithm based on mutual information (MI) for MIMO radar target tracking was derived using wideband orthogonal frequency division multiplexing (OFDM) signaling scheme. In [24], [25] an optimal waveform design technique based on minimum MSE (MMSE) of a single target location estimation and minimum validation gate using the conventional Kalman filter was derived. In [26], this method was generalized to account for multiple maneuvering target tracking. In [27] an optimal waveform design based on minimization of the MSE of moving target location estimation was proposed for linear Gaussian state model and a nonlinear Gaussian measurement model.

The cognitive beamforming algorithm presented in [17] demonstrated that in an array configuration with ambiguity nature, the RMB-based beamforming optimization produces superior target parameter estimation performance over the BCRB-based optimization. In identical transmit and receive arrays the target parameter estimation performance of the RMB-based optimization and the BCRB-based optimization coincide. Furthermore, the non-convexity of the RMB-based optimization criterion introduces additional computational complexity.

In this paper, we propose a cognitive beamforming algorithm for moving target tracking in the presence of environmental uncertainties. We consider a linear Markovian state model which represents the dynamics of the target and variations of the environmental unknown random parameters over time. The observation model is a non-linear function of the unknown parameters contaminated by additive Gaussian noise. The proposed target tracking algorithm is applied using sequential Bayesian filtering, implemented by particle filtering [28]–[34]. The optimization of the transmit beampattern in [17] is extended to account for target dynamics and environmental uncertainties. For this purpose, the sequential conditional BCRB (CBCRB) [36]–[38] is chosen as an optimization criterion. It is shown, that the computational complexity of the sequential CBCRB increases quadratically with the number of pulse steps. Therefore, an approximation of the bound, which reduces the computational complexity, is presented. At each step, the system parameters are estimated by using the MMSE estimator that is implemented using the probability density function (pdf) of the target parameters given all the history observations. The results in this work demonstrate the advantage of the proposed cognitive algorithm for transmit beamforming over non-cognitive beamforming in the presence of environmental uncertainties, in terms of the performance of dynamic target location estimation.

The rest of this paper is organized as follows. In Section II, the system state model and cognitive MIMO signal model for a moving target and environmental uncertainties are presented. In Section III, we present the sequential CBCRB and the approximated sequential CBCRB for estimation performance of a dynamic system as a measure for optimization, and provide tools for computing the sequential CBCRB. In Section IV, an optimization scheme is presented. In Section V, simulations results of a dynamic target in a realistic underwater waveguide with unknown channel uncertainties are reported. Our conclusions appear in Section VI.

## II. Dynamic Target and MIMO Radar/Sonar Model

Consider a colocated MIMO radar/sonar transmitting narrowband signals in a dynamic target scenario. The following general observation model describes a colocated MIMO system of $N_T$ transmitters and $N_R$ receivers:

$$\mathbf{x}_k[l] = \alpha_k \mathbf{a}_R(\boldsymbol{\varphi}_k)\mathbf{a}_T^T(\boldsymbol{\varphi}_k)\mathbf{s}_k[l] + \mathbf{n}_k[l], \quad l = 1,\ldots,L, k = 1,2,\ldots \tag{1}$$

where $\mathbf{x}_k[l] \in \mathbb{C}^{N_R}$, $\mathbf{s}_k[l] \in \mathbb{C}^{N_T}$, and $\mathbf{n}_k[l] \in \mathbb{C}^{N_R}$ denote the $l$th snapshot at the $k$th pulse of the observation, the transmit signal, and the noise vector, respectively. $L$ is the number of total snapshots in each pulse step, $\alpha_k \in \mathbb{C}$ and $\boldsymbol{\varphi}_k \in \mathbb{R}^{N_\varphi}$ represent the complex attenuation factor and the vector of target location and environmental parameters at the $k$th pulse step, respectively. The terms $\mathbf{a}_R(\cdot) \in \mathbb{C}^{N_R}$ and $\mathbf{a}_T(\cdot) \in \mathbb{C}^{N_T}$ represent the steering vectors of the receive and transmit arrays, respectively. Denote the vector $\boldsymbol{\theta}_k \in \mathbb{R}^{N_\theta}$ as the system state vector, which is assumed to be random with initial *a-priori* distribution function $f_{\boldsymbol{\theta}_0}$, defined by $\boldsymbol{\theta}_k \triangleq [\mathrm{Re}(\alpha_k), \mathrm{Im}(\alpha_k), \boldsymbol{\varphi}_k^T]^T$, where $\mathrm{Re}(\cdot)$ and $\mathrm{Im}(\cdot)$ denote the real and imaginary part of their argument, respectively.

In this paper, we consider the particular case of unobserved first-order Markovian linear state model, often used in target tracking problems. The state and observation models pair is given by

$$\begin{aligned} \boldsymbol{\theta}_k &= \mathbf{F}_k\boldsymbol{\theta}_{k-1} + \mathbf{u}_k \\ \mathbf{X}_k &= \mathbf{H}(\boldsymbol{\theta}_k)\mathbf{S}_k + \mathbf{N}_k \end{aligned} \tag{2}$$

where the state noise process $\{\mathbf{u}_k\}$ is assumed to be independent and identically distributed (i.i.d.) real Gaussian sequence of random vectors with zero mean and known covariance matrix, $\mathbf{R}_\mathbf{u}$. The measurement, transmit signal, and measurement noise matrices are given by $\mathbf{X}_k = [\mathbf{x}_k[1],\ldots,\mathbf{x}_k[L]]$, $\mathbf{S}_k = [\mathbf{s}_k[1],\ldots,\mathbf{s}_k[L]]$, and $\mathbf{N}_k = [\mathbf{n}_k[1],\ldots,\mathbf{n}_k[L]]$, respectively. We assume that the columns of $\mathbf{N}_k$ are i.i.d. complex circularly symmetric Gaussian random vectors with zero-mean and known covariance matrix, $\mathbf{R}$. The matrix $\mathbf{H}(\boldsymbol{\theta}_k) \triangleq \alpha_k \mathbf{a}_R(\boldsymbol{\varphi}_k)\mathbf{a}_T^T(\boldsymbol{\varphi}_k)$ denotes the MIMO channel matrix.

Fig. 1 describes the cognitive system for the case of a dynamic system state. In each step, an optimal transmit beampattern is derived based on the state vector and previous measurements, such that a chosen criterion is optimized. The state vector estimate is given by $\hat{\boldsymbol{\theta}}_k$. In this work, we consider the target tracking problem in which at each step the transmit beampattern adaptively optimizes the expected estimation performance of $\boldsymbol{\theta}_k$ in terms of MMSE. The MMSE is computationally intractable and therefore, the optimization criterion will be based on a lower bound on the MSE. Specifically, we will employ the sequential CBCRB as will be described in the next section.

## III. Recursive Computation of the Conditional BCRB in a Dynamic System

Sequential computation of the conventional BCRB and the CBCRB for dynamic system state vector estimation have been introduced in [36], [37], and [38], respectively. In this section, we derive the recursive algorithm for computing the CBCRB,

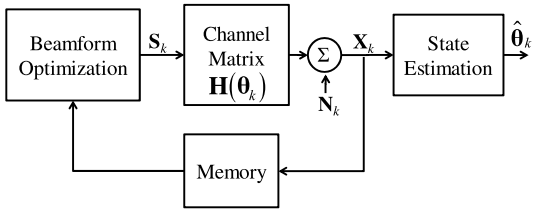


Fig. 1. Cognitive scheme for dynamic system state with additive noise.

for the dynamic system model presented in the previous section. At each step, the algorithm sequentially calculates the CBCRB for estimating the current state vector, which is dependent of the transmit autocorrelation matrix at the current step. In the following, we first present the exact sequential CBCRB given history observations. Then, we present an approximation for the sequential CBCRB, in order to reduce the computational complexity in comparison to the exact sequential CBCRB.

### *A. The Sequential Conditional BCRB for Estimating Dynamic Model State Vector*

In this subsection, the sequential CBCRB [38] is presented. Define $\boldsymbol{\theta}^{(k)} \triangleq [\boldsymbol{\theta}_0^T, \ldots, \boldsymbol{\theta}_k^T]^T$ and $\mathbf{X}^{(k)} \triangleq [\mathbf{X}_1, \ldots, \mathbf{X}_k]$ as the unknown state vector sequence and the observation sequence up to the $k$th step, respectively, and let $\mathbf{J}_{\boldsymbol{\theta}^{(k)}}(\mathbf{X}^{(k-1)}) \in \mathbb{R}^{(k+1)N_\theta \times (k+1)N_\theta}$ denote the conditional Bayesian Fisher information matrix (CBFIM) for estimating $\boldsymbol{\theta}^{(k)}$ based on the joint conditional pdf $f_{\boldsymbol{\theta}^{(k)}, \mathbf{X}_k | \mathbf{X}^{(k-1)}}$. Therefore, the lower bound for the predicted MMSE estimation of $\boldsymbol{\theta}^{(k)}$ using the observations $\mathbf{X}^{(k)}$, namely the CBCRB, is given by $\mathbf{C}_{\boldsymbol{\theta}^{(k)}}(\mathbf{X}^{(k-1)}) \triangleq \mathbf{J}^{-1}_{\boldsymbol{\theta}^{(k)}}(\mathbf{X}^{(k-1)})$.

Denote $\mathbf{C}_{\boldsymbol{\theta}_i}(\mathbf{X}^{(k-1)}) \in \mathbb{R}^{N_\theta \times N_\theta}$, $i = 1, \ldots, k$, as the CBCRB for estimating $\boldsymbol{\theta}_i$ from $\mathbf{X}^{(k)}$ conditioned on the observations $\mathbf{X}^{(k-1)}$, which is given by the $i$th diagonal block of the CBCRB, $\mathbf{C}_{\boldsymbol{\theta}^{(k)}}(\mathbf{X}^{(k-1)})$. Define $\mathbf{J}_{\boldsymbol{\theta}_i}(\mathbf{X}^{(k-1)}) \in \mathbb{R}^{N_\theta \times N_\theta}$ as the corresponding equivalent CBFIM, given by $\mathbf{J}_{\boldsymbol{\theta}_i}(\mathbf{X}^{(k-1)}) \triangleq \mathbf{C}^{-1}_{\boldsymbol{\theta}_i}(\mathbf{X}^{(k-1)})$, which takes into account the lack of knowledge of the whole vector $\boldsymbol{\theta}^{(k)}$.

In the Appendix, it is shown that the equivalent CBFIM of estimating $\boldsymbol{\theta}_i$, $i = 1, \ldots, k$ can be sequentially calculated as follows

$$\mathbf{J}_{\boldsymbol{\theta}_i}\left(\mathbf{X}^{(k-1)}\right) = \mathbf{J}_{P_{i-1}}\left(\mathbf{X}^{(k-1)}\right) + \triangle\mathbf{J}_{\boldsymbol{\theta}_i}\left(\mathbf{X}^{(k-1)}\right), \quad i = 1, \ldots, k \tag{3}$$

where $\mathbf{J}_{\boldsymbol{\theta}_0}(\mathbf{X}^{(k-1)}) \triangleq -\mathrm{E}[(\partial^2 \log f_{\boldsymbol{\theta}_0}/\partial\boldsymbol{\theta}_0^2)|\mathbf{X}^{(k-1)}]$, the gradient operator is defined by $d/d\boldsymbol{\gamma} \triangleq [(\partial/\partial\gamma_1), \ldots, (\partial/\partial\gamma_{N_\gamma})]$, the second order gradient is defined by $d^2/d\boldsymbol{\gamma}^2 \triangleq (d/d\boldsymbol{\gamma})[d/d\boldsymbol{\gamma}]^T$, and $\mathbf{J}_{P_{i-1}}(\mathbf{X}^{(k-1)})$ is the equivalent CBFIM due to the statistical information from history, defined in [38] as follows

$$\begin{aligned}\mathbf{J}_{P_{i-1}}&\left(\mathbf{X}^{(k-1)}\right) \\ &= \mathbf{R}_{\mathbf{u}}^{-1} - \mathbf{R}_{\mathbf{u}}^{-1}\mathbf{F}_i \\ &\quad \times \left[\mathbf{J}_{\boldsymbol{\theta}_{i-1}}\left(\mathbf{X}^{(k-1)}\right) + \mathbf{F}_i^T\mathbf{R}_{\mathbf{u}}^{-1}\mathbf{F}_i\right]^{-1}\mathbf{F}_i^T\mathbf{R}_{\mathbf{u}}^{-1}, \\ &\quad i = 1, \ldots, k\end{aligned} \tag{4}$$

and the matrix $\triangle\mathbf{J}_{\boldsymbol{\theta}_i}(\mathbf{X}^{(k-1)})$ denotes the incremental CBFIM for estimating $\boldsymbol{\theta}_i$, given by

$$\begin{aligned}&\triangle\mathbf{J}_{\boldsymbol{\theta}_i}\left(\mathbf{X}^{(k-1)}\right) \\ &\quad \triangleq -\mathrm{E}\left[\frac{\partial^2 \log f_{\mathbf{X}_i|\boldsymbol{\theta}_i}}{\partial\boldsymbol{\theta}_i^2}\middle| \mathbf{X}^{(k-1)}\right] \\ &\quad = 2L\mathrm{Re}\left\{\mathbf{V}_{N_\theta}\left[\boldsymbol{\Gamma}_{\boldsymbol{\theta}_i}\left(\mathbf{X}^{(k-1)}\right) \odot \left[\mathbf{1}_{N_\theta \times N_\theta} \otimes \mathbf{R}_{\mathbf{s}_i}^T\right]\right]\mathbf{V}_{N_\theta}^T\right\}, \\ &\quad i = 1, \ldots, k\end{aligned} \tag{5}$$

where $\mathbf{R}_{\mathbf{s}_i} \triangleq (1/L)\mathbf{S}_i\mathbf{S}_i^H$ denotes the $i$th step transmit autocorrelation matrix and $\boldsymbol{\Gamma}_{\boldsymbol{\theta}_i}$ is given by

$$\boldsymbol{\Gamma}_{\boldsymbol{\theta}_i}\left(\mathbf{X}^{(k-1)}\right) \triangleq \mathrm{E}\left[\dot{\mathbf{H}}^H(\boldsymbol{\theta}_i)\mathbf{R}^{-1}\dot{\mathbf{H}}(\boldsymbol{\theta}_i)\middle| \mathbf{X}^{(k-1)}\right] \tag{6}$$

where $\dot{\mathbf{H}}(\boldsymbol{\theta}) \triangleq [(\partial\mathbf{H}/\partial\theta_1), \ldots, (\partial\mathbf{H}/\partial\theta_{N_\theta})]$. The matrix $\mathbf{1}_{N_\theta \times N_\theta}$ is an $N_\theta \times N_\theta$ matrix whose entries are equal to one, $\mathbf{V}_{N_\theta} \triangleq \mathbf{I}_{N_\theta} \otimes \mathbf{1}_{1 \times N_T}$, and the operators $\odot$ and $\otimes$ are the Hadamard product and the Kronecker product, respectively. The expectation in (6) is performed w.r.t. the conditional pdf $f_{\boldsymbol{\theta}_i|\mathbf{X}^{(k-1)}}$ in the $i$th step of the recursion. Note that new measurements provide new information about the system state in the past, which requires to perform the entire sequential calculation in (3) at each step $k$. Therefore, the computational complexity for calculating the CBCRB, $\mathbf{C}_{\boldsymbol{\theta}_k}(\mathbf{X}^{(k-1)})$, linearly increases with the pulse step index $k$, since at the $k$th step, the recursive equation in (3) is performed $k$ times.

In order to decrease the amount of the computations in (3), we propose to approximate the sequential CBCRB [38] as follows. The sequential CBCRB can be approximated by taking the expectations in (6) w.r.t. the state *prediction* pdf $f_{\boldsymbol{\theta}_i|\mathbf{X}^{(i-1)}}$ for $i = 1, \ldots, k$, instead of the conditional pdfs $f_{\boldsymbol{\theta}_i|\mathbf{X}^{(k-1)}}$. Denote $\mathbf{J}'_{\boldsymbol{\theta}_k}(\mathbf{X}^{(k-1)}) \in \mathbb{R}^{N_\theta \times N_\theta}$ as the approximated equivalent CBFIM for estimating $\boldsymbol{\theta}_k$ conditioned on the observations $\mathbf{X}^{(k-1)}$. The term $\mathbf{J}'_{\boldsymbol{\theta}_k}(\mathbf{X}^{(k-1)})$ satisfies the following recursive equation

$$\mathbf{J}'_{\boldsymbol{\theta}_k}\left(\mathbf{X}^{(k-1)}\right) = \mathbf{J}'_{P_{k-1}}\left(\mathbf{X}^{(k-2)}\right) + \triangle\mathbf{J}_{\boldsymbol{\theta}_k}\left(\mathbf{X}^{(k-1)}\right) \tag{7}$$

where $\mathbf{J}'_{P_{k-1}}(\mathbf{X}^{(k-2)})$ is the approximation of the equivalent CBFIM due to the statistical information from history, given by

$$\begin{aligned}\mathbf{J}'_{P_{k-1}}&\left(\mathbf{X}^{(k-2)}\right) = \mathbf{R}_{\mathbf{u}}^{-1} - \mathbf{R}_{\mathbf{u}}^{-1}\mathbf{F}_k \\ &\quad \times \left[\mathbf{J}'_{\boldsymbol{\theta}_{k-1}}\left(\mathbf{X}^{(k-2)}\right) + \mathbf{F}_k^T\mathbf{R}_{\mathbf{u}}^{-1}\mathbf{F}_k\right]^{-1}\mathbf{F}_k^T\mathbf{R}_{\mathbf{u}}^{-1}.\end{aligned} \tag{8}$$

The difference between the exact equivalent CBFIM $\mathbf{J}_{\boldsymbol{\theta}_k}(\mathbf{X}^{(k-1)})$ in (3) and its approximation in (7) is the use of $\mathbf{J}'_{\boldsymbol{\theta}_{k-1}}(\mathbf{X}^{(k-2)})$ instead of $\mathbf{J}_{\boldsymbol{\theta}_{k-1}}(\mathbf{X}^{(k-1)})$ in the recursive equation. The computational complexity for calculating the approximate CBCRB, given by $\mathbf{C}'_{\boldsymbol{\theta}_k}(\mathbf{X}^{(k-1)}) \triangleq \mathbf{J}'^{-1}_{\boldsymbol{\theta}_k}(\mathbf{X}^{(k-1)})$, is constant w.r.t. the pulse step index $k$, since at the $k$th step the recursion in (7) is performed only once. Note that there is an inherent error which propagates in the recursion, due to the approximation. However, in common scenarios this error is insignificant, as will be demonstrated via simulations in Section V.

### B. Recursive Computation of the Conditional PDF

Equation (6) involves the calculation of expectations w.r.t. the conditional pdfs $f_{\boldsymbol{\theta}_i|\mathbf{X}^{(k-1)}}$ for $i=1,\ldots,k$, at the $k$th step. In addition, the MMSE estimator of $\boldsymbol{\theta}_k$ at the $k$th step requires performing expectation w.r.t. the state *posterior* pdf $f_{\boldsymbol{\theta}_k|\mathbf{X}^{(k)}}$. Since the observation model in (2) is non-linear, calculation of $f_{\boldsymbol{\theta}_i|\mathbf{X}^{(k-1)}}$ for $i=1,\ldots,k$ is intractable. In this subsection, we will use a Monte-Carlo (MC) based method for computation of the expectations, as well as for approximating the conditional pdf.

The expectations can be computed using the MC integration method, where $N_s$ samples of the above mentioned pdfs are sequentially obtained by using Bayesian bootstrap methods [34] and particle filtering (PF) tracking methods [28]–[33]. At the $k$th step, the state *posterior* pdf $f_{\boldsymbol{\theta}_k|\mathbf{X}^{(k)}}$ can be approximated via PF tracking algorithm. Computation of $f_{\boldsymbol{\theta}_0|\mathbf{X}^{(0)}}$ is performed by generating particles (samples) from the *a-priori* pdf $f_{\boldsymbol{\theta}_0}$. Then, the so called *proposal density function* and *importance density function* are chosen as the transition pdf $f_{\boldsymbol{\theta}_k|\boldsymbol{\theta}_{k-1}}$ and the observation pdf $f_{\mathbf{X}_k|\boldsymbol{\theta}_k}$, respectively. In the case of system equations as in (2), the observation and the transition distributions are given by $\mathbf{X}_k|\boldsymbol{\theta}_k \sim CN(\mathbf{H}(\boldsymbol{\theta}_k)\mathbf{S}_k,\mathbf{R})$ and $\boldsymbol{\theta}_k|\boldsymbol{\theta}_{k-1} \sim N(\mathbf{F}_k\boldsymbol{\theta}_{k-1},\mathbf{R}_{\mathbf{u}})$, respectively. In this work, we employed the auxiliary particle filter (APF) [31], [32] as a MC based method for approximating the state *posterior* pdf.

Samples of the conditional pdf $f_{\boldsymbol{\theta}_i|\mathbf{X}^{(k-1)}}$ for $i=1,\ldots,k-2,k$ are obtained using filtering and reverse-filtering algorithms. Assume we have samples representing the $(k-1)$th step state *posterior* pdf $f_{\boldsymbol{\theta}_{k-1}|\mathbf{X}^{(k-1)}}$. Then, by using the Bayesian bootstrap filter [34], [35] we produce samples representing the predicted state pdf $f_{\boldsymbol{\theta}_k|\mathbf{X}^{(k-1)}}$ by applying the state model equation in (2) for each sample. Using a similar approach, samples from each conditional pdf $f_{\boldsymbol{\theta}_i|\mathbf{X}^{(k-1)}}$ for $i=1,\ldots,k-2$ can be obtained by propagating each sample according to the reversed transition pdf $f_{\boldsymbol{\theta}_{k-1}|\boldsymbol{\theta}_k}$.

The sequential algorithm for calculating the conditional pdfs is concluded in Table I.

TABLE I
SEQUENTIAL ALGORITHM FOR COMPUTING THE CONDITIONAL PDFS

1. Initialization:
   Set $k=0$, $f_{\boldsymbol{\theta}_0|\mathbf{X}^{(0)}}=f_{\boldsymbol{\theta}_0}$. Generate $N_s$ samples (particles) representing the initial distribution $f_{\boldsymbol{\theta}_0}$.
   Set $k=1$, produce the 1st step set of predicted state pdf samples which approximate the state-prediction pdf $f_{\boldsymbol{\theta}_1|\mathbf{X}^{(0)}}$, by passing each sample representing the initial distribution through the state model.
2. Obtain the $k$th step observation $\mathbf{X}_k$ based on the observation model in (2), and obtain $f_{\mathbf{X}_k|\boldsymbol{\theta}_k}$ analytically.
3. Produce the $k$th step set of samples (particles) which approximate the state *posterior* pdf $f_{\boldsymbol{\theta}_k|\mathbf{X}^{(k)}}$, by applying the APF with the proposal distribution $f_{\boldsymbol{\theta}_k|\boldsymbol{\theta}_{k-1}}$ and importance density function $f_{\mathbf{X}_k|\boldsymbol{\theta}_k}$.
4. Produce the $(k+1)$th step set of predicted state pdf samples which approximate the state-prediction pdf $f_{\boldsymbol{\theta}_{k+1}|\mathbf{X}^{(k)}}$, by passing each sample from the $k$th step through the state model.
5. Set $i=k-1$ and perform the following loop:
   WHILE $i \geq 0$
   - Produce the $i$th step conditional pdf samples which approximate the conditional pdf $f_{\boldsymbol{\theta}_i|\mathbf{X}^{(k)}}$, by passing each sample through the reversed transition function.
   - $i=i-1$.

   END WHILE
6. Set $k=k+1$ and repeat from step 2.

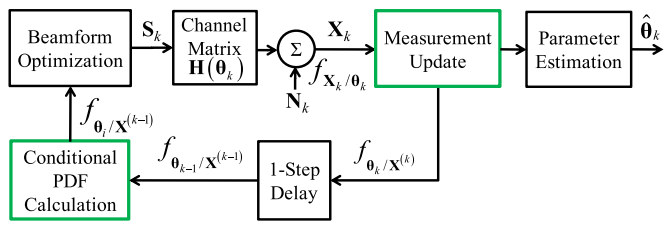


Fig. 2. The adaptive transmit beamforming algorithm.

## IV. Optimal Cognitive Beamforming

In this section, we propose a method for adaptive transmit beamforming for the state and observation models presented in Section II. The adaptive method extends the method in [17], with the extension to the case of dynamic system model in the presence of environmental uncertainties. At each step, the algorithm determines the transmit beampattern in order to optimize the estimation performance in terms of a chosen criterion. The optimization criterion is based on the sequential CBCRB or its approximation presented in the previous section, for estimating the state vector. In Fig. 2 we present the adaptive scheme for beamform optimization. We assume that the state vector consists of target parameters and uncertain environmental parameters. The optimization problem is defined such that the performance bound for estimating the target parameters is optimized. For simplicity of presentation the notations in the following refer to the exact sequential CBCRB based criterion. For approximated sequential CBCRB, $\mathbf{J}'_{\boldsymbol{\theta}_k}(\mathbf{X}^{(k-1)})$ from (7), should be used instead of $\mathbf{J}_{\boldsymbol{\theta}_k}(\mathbf{X}^{(k-1)})$ from (3).

### A. Optimization Problem Formulation

The transmit beamforming is performed by finding transmit signal, $\mathbf{S}_k^{(opt)}$, which optimizes a given criterion, based on previous observations $\mathbf{X}^{(k-1)}$. The sequential CBCRB for estimating $\boldsymbol{\theta}_k$ in (3) utilizes knowledge from history observation, and is a suitable measure for estimation performance in cognitive systems in terms of MMSE.

Assume that the state vector $\boldsymbol{\theta}_k$ can be described as $\boldsymbol{\theta}_k = [\boldsymbol{\theta}_{tgt_k}^T, \boldsymbol{\theta}_{env_k}^T]^T$, where the vectors $\boldsymbol{\theta}_{tgt_k} \in \mathbb{R}^{N_{tgt}}$ and $\boldsymbol{\theta}_{env_k} \in \mathbb{R}^{N_{env}}$ represent the unknown target and environmental parameters at the $k$th step, respectively. Let $\mathbf{C}_{\boldsymbol{\theta}_k}(\mathbf{X}^{(k-1)})$ denote the sequential CBCRB, given by the inverse of the equivalent CBFIM $\mathbf{J}_{\boldsymbol{\theta}_k}(\mathbf{X}^{(k-1)})$. Considering the definition of $\boldsymbol{\theta}_{tgt_k}$ and $\boldsymbol{\theta}_{env_k}$ above, the top left $N_{tgt} \times N_{tgt}$ block of $\mathbf{C}_{\boldsymbol{\theta}_k}(\mathbf{X}^{(k-1)})$ relates to the sequential CBCRB for estimating the target parameters $\boldsymbol{\theta}_{tgt_k}$.

The equivalent sequential CBFIM from (3) is a function of the transmit signal only through the transmit autocorrelation matrix $\mathbf{R}_{\mathbf{s}_k}$. Therefore, the aim of the optimization is to find an optimal transmit autocorrelation matrix $\mathbf{R}_{\mathbf{S}_k}^{(opt)}$, such that the criterion is optimized given transmit signal energy constraints. Consider the total energy constraint in which the total energy transmitted from all the transmitters, is limited to $P$. The constraint is defined as $\mathrm{tr}(\mathbf{R}_{\mathbf{s}_k}) \leq P$. In some radar/sonar applications, each transmitter may have limited energy output $P_j$. In such case,

the constraint may be defined as $[\mathbf{R}_{\mathbf{s}_k}]_{jj} \leq P_j,\ j = 1, \ldots, N_T$, where $\sum_{j=1}^{N_T} P_j = P$. It can be seen that both sets of constraints are convex. In this paper, we will consider the total power limit constraint.

The sequential CBCRB $\mathbf{C}_{\boldsymbol{\theta}_k}(\mathbf{X}^{(k-1)})$ is a matrix, and thus several optimization criteria can be chosen, such as minimization of the weighted trace, the determinant, or the largest eigenvalue of the sequential CBCRB, w.r.t. the transmit autocorrelation matrix. According to (3) and (5) the CBFIM is a linear function of the transmit autocorrelation matrix $\mathbf{R}_{\mathbf{s}_k}$. Therefore, the criteria mentioned above with the constraints $\mathrm{tr}(\mathbf{R}_{\mathbf{s}_k}) \leq P$ and $\mathbf{R}_{\mathbf{s}_k} \succeq 0$, lead to a convex optimization problems [46], which can be solved efficiently using interior point methods [47],[48]. Practically, the optimization problems can be computed using common optimization problem solvers, such as [52].

In this work, we will consider the criterion of weighted trace minimization of the matrix $\mathbf{C}_{\boldsymbol{\theta}_k}(\mathbf{X}^{(k-1)})$. Accordingly, the optimization problem can be stated as

$$\begin{aligned} \mathbf{R}_{\mathbf{s}_k}^{(opt)} &= \arg\min_{\mathbf{R}_{\mathbf{s}_k}} \mathrm{tr}\left(\mathbf{W}\mathbf{C}_{\boldsymbol{\theta}_k}\left(\mathbf{X}^{(k-1)}\right)\right) \\ &\text{s.t. } \mathrm{tr}\left(\mathbf{R}_{\mathbf{s}_k}\right) \leq P, \mathbf{R}_{\mathbf{s}_k} \succeq 0 \end{aligned} \tag{9}$$

where $\mathbf{W} = \mathrm{diag}(w_1, \ldots, w_{N_\theta})$ is a positive semi-definite weighting matrix. Assuming that we are interested in the target parameters $\boldsymbol{\theta}_{tgt_k}$ only, then the weights corresponding to the environmental parameters are set to zero, that is $w_j = 0,\ j = N_{tgt} + 1, \ldots, N_\theta$. In [47], [48] it was shown that the optimization problem in (9) can be transformed into the following SDP problem:

$$\begin{aligned} \mathbf{R}_{\mathbf{s}_k}^{(opt)} &= \arg\min_{\mathbf{R}_{\mathbf{s}_k}} \left[\min_{\{t_i\}} \sum_{i=1}^{N_{tgt}} w_i t_i\right] \\ &\text{s.t. } \begin{bmatrix} \mathbf{J}_{\boldsymbol{\theta}_k}\left(\mathbf{X}^{(k-1)}\right) & \mathbf{e}_i \\ \mathbf{e}_i^T & t_i \end{bmatrix} \succeq 0,\ i = 1, \ldots, N_{tgt} \\ &\mathrm{tr}\left(\mathbf{R}_{\mathbf{s}_k}\right) \leq P, \mathbf{R}_{\mathbf{s}_k} \succeq 0 \end{aligned} \tag{10}$$

where the vector $\mathbf{e}_i$ is the $i$th column of the identity matrix of size $N_\theta$, $\{t_i\}_{i=1}^{N_{tgt}}$ are auxiliary variables, and $\mathbf{J}_{\boldsymbol{\theta}_k}(\mathbf{X}^{(k-1)})$ is defined in (7). The expectations for computing $\boldsymbol{\Gamma}_{\boldsymbol{\theta}_k}(\mathbf{X}^{(k-1)})$ in (5) are performed w.r.t. the state *prediction* pdf $f_{\boldsymbol{\theta}_k|\mathbf{X}^{(k-1)}}$. Note that the constraints in the above SDP are either linear matrix inequalities (LMIs) or linear inequalities in the elements of $\mathbf{R}_{\mathbf{s}_k}$.

The proposed adaptive transmit beamforming algorithm for target tracking in the presence of environmental uncertainties is concluded in Table II.

TABLE II
ADAPTIVE TRANSMIT BEAMFORMING ALGORITHM

1. Set $k = 0$, $f_{\boldsymbol{\theta}_0|\mathbf{X}^{(0)}} = f_{\boldsymbol{\theta}_0}$. Generate $N_s$ particles representing the initial distribution $f_{\boldsymbol{\theta}_0}$. Set $k = 1$.
2. Generate a set of $N_s$ samples which approximate the conditional pdfs $f_{\boldsymbol{\theta}_i|\mathbf{X}^{(k-1)}},\ i = 1, \ldots, k$, using Bayesian bootstrap methods.
3. Calculate $\boldsymbol{\Gamma}_{\boldsymbol{\theta}_i}\left(\mathbf{X}^{(k-1)}\right),\ i = 1, \ldots, k$ using MC integration with the set of samples obtained in step 2.
4. Calculate the equivalent CBFIM $\mathbf{J}_{\boldsymbol{\theta}_k}\left(\mathbf{X}^{(k-1)}\right)$ according to (3).
5. Find $\mathbf{R}_{\mathbf{S}_k}^{(opt)}$ by solving the SDP problem in (10).
6. Obtain $\mathbf{S}_k^{(opt)}$ from $\mathbf{R}_{\mathbf{S}_k}^{(opt)}$, and obtain the $k$th observation $\mathbf{X}_k$ using (2).
7. Generate a set of $N_s$ samples which represent the state *posterior* pdf $f_{\boldsymbol{\theta}_k|\mathbf{X}^{(k)}}$ at the $k$th step, by applying the APF on the set of state *posterior* samples from the $(k-1)$th step.
8. Obtain the MMSE estimator $\hat{\boldsymbol{\theta}}_k\left(\mathbf{X}^{(k)}\right) = \mathrm{E}\left[\boldsymbol{\theta}_k|\,\mathbf{X}^{(k)}\right]$ by using the MC integration with the set of samples obtained in step 6.
9. Set $k = k + 1$ and repeat from step 2.

### B. Computational Complexity Analysis

In this subsection, we analyze the computational complexity of the proposed adaptive algorithm at the $k$th step, for the exact sequential CBCRB from (3) and its approximation from (7) as optimization criteria.

According to Table II, the computational complexity of the adaptive algorithm based on the exact sequential CBFIM $\mathbf{J}_{\boldsymbol{\theta}_k}(\mathbf{X}^{(k-1)})$ from (3) as the optimization criterion is approximately equal to the summation of the following factors. Samples from the conditional pdf's $f_{\boldsymbol{\theta}_i|\mathbf{X}^{(k-1)}},\ i = 1, \ldots, k$ (step 2 in Table II), are produced using Bayesian bootstrap methods in which each of the $N_s$ samples representing the $(k-1)$th step state *posterior* pdf is propagated through the state model equations. Therefore, the number of operations for computing each conditional pdf is approximately $\mathcal{O}(N_\theta^2 N_s)$, which results from summation of $N_\theta^2$ matrix products over $N_s$ samples. The expectations in $\boldsymbol{\Gamma}_{\boldsymbol{\theta}_i}(\mathbf{X}^{(k-1)}),\ i = 1, \ldots, k$ (step 3 in Table II) are performed using MC integrations. The amount of computations for each MC integration is approximately $\mathcal{O}(N_s N_R N_T^2 N_\theta^2)$ [51]. The calculation of $\mathbf{J}_{\boldsymbol{\theta}_k}(\mathbf{X}^{(k-1)})$ from (3) (step 4 in Table II) requires $k$ calculations of $\boldsymbol{\Gamma}_{\boldsymbol{\theta}_i}(\mathbf{X}^{(k-1)}),\ i = 1, \ldots, k$ and $k$ matrix inversions. The amount of computations for a standard matrix inversion is approximately $\mathcal{O}(N_\theta^3)$. Therefore, the number of operations for calculation of $\mathbf{J}_{\boldsymbol{\theta}_k}(\mathbf{X}^{(k-1)})$ is $k\mathcal{O}(N_s N_R N_T^2 N_\theta^2) + k\mathcal{O}(N_\theta^3)$. The number of operations required for solving the SDP problem in (10) (step 5 in Table II) is [46] $\mathcal{O}(\sqrt{\log N_T})$. The computation of state*posterior* pdf at the $k$th step (step 7 in Table II) is performed via APF on $N_s$ samples from the $(k-1)$th step. The APF consists of performing prediction, weighting the predicted samples according to the *importance density function*, resampling the predicted samples, and measurement update (see e.g. [30], [31], [33]). The complexity of the prediction is $\mathcal{O}(N_\theta^2 N_s)$ which results from propagating the $N_s$ samples of the *posterior* from the $(k-1)$th step through the noiseless state model. The importance weighting is performed by employing the observation pdf on the $N_s$ predicted samples with normalization, with complexity of $\mathcal{O}(N_s N_R N_T L + N_s N_R^2 L)$. The amount of computations at the resampling is $\mathcal{O}(N_s)$ [30], [31], [33]. The measurement update is performed by employing the state model on the $N_s$ resampled predicted samples, with number of operations of order $\mathcal{O}(N_\theta^2 N_s)$. Therefore, the number of operations of the APF is approximately $\mathcal{O}(N_s N_\theta^2 + N_s N_R N_T L + N_s N_R^2 L)$. The MMSE estimator (step 8 in Table II) is obtained by using the MC integration over the $N_s$ samples of the state *posterior* pdf with computational complexity of $\mathcal{O}(N_s N_R N_T^2 N_\theta^2)$. Consequently, the total computational complexity at the $k$th step of the adaptive algorithm due to significant factors when $\mathbf{J}_{\boldsymbol{\theta}_k}(\mathbf{X}^{(k-1)})$ from (3) is used as the optimization criterion, is given by

$k\mathcal{O}(N_sN_RN_T^2N_\theta^2)+k\mathcal{O}(N_\theta^3)+\mathcal{O}(N_sN_\theta^2+N_sN_RN_TL+N_sN_R^2L)$.

The computational complexity analysis of the adaptive algorithm based on the approximation $\mathbf{J}'_{\boldsymbol{\theta}_k}(\mathbf{X}^{(k-1)})$ from (7) as the optimization criterion, differs from the aforementioned computational complexity analysis in the following factors. Step 2 in Table II requires the computation of the state *prediction* pdf only, which is performed once at the $k$th step. Step 3 in Table II requires the computation of the expectation $\boldsymbol{\Gamma}_{\boldsymbol{\theta}_k}(\mathbf{X}^{(k-1)})$ using a single MC integration. Step 4 in Table II consists of the computation of the approximation $\mathbf{J}'_{\boldsymbol{\theta}_k}(\mathbf{X}^{(k-1)})$, which requires the calculation of $\boldsymbol{\Gamma}_{\boldsymbol{\theta}_k}(\mathbf{X}^{(k-1)})$ and a single matrix inversion. Summing up the aforementioned factors, the number of operations due to the significant factors at the $k$th step is of order $\mathcal{O}(N_sN_RN_T^2N_\theta^2)+\mathcal{O}(N_\theta^3)+\mathcal{O}(N_sN_\theta^2+N_sN_RN_TL+N_sN_R^2L)$. The difference of the adaptive algorithm run-time between two optimization criteria is demonstrated via simulations in Section V.

## V. Simulations—Application to Target Tracking in Shallow Underwater Channels

In this section, we evaluate the performance of the proposed adaptive beamforming method for target tracking in a shallow underwater environment. Underwater localization of a point source has been studied in several works (see e.g. [39]–[45]) and various underwater target localization approaches, such as matched-field processing (MFP) [41], [42] and maximum likelihood (ML) localization [39], have been introduced. Several performance analysis studies, such as the Cramér-Rao bound [39], [40], [42] for source localization in underwater waveguides were performed. Source localization in a shallow water waveguide in the presence of environmental uncertainties has been studied in several works (see e.g. [40], [41], [44]).

Consider an active MIMO sonar system presented in Fig. 3, with colocated transmit and receive vertical arrays, located in a time-invariant non-homogenous waveguide, referred as the Pekeris waveguide [55], such that the propagation model can be described by normal-modes [39], [41], [43], [44]. A point target is located in the waveguide at depth $z_k$ and range $r_k$ from vertical arrays of omnidirectional transmit and receive elements, at the $k$th step. Denote the target location vector at the $k$th step by $[z_k, r_k]^T$ and its complex attenuation factor by $\alpha_k$. The transmit and receive elements are located at $\{z_{T_i}\}_{i=1}^{N_T}$ and $\{z_{R_i}\}_{i=1}^{N_R}$, respectively, where $z_{T_i}$ and $z_{R_i}$ are the depths of the $i$th element of the transmit and receive arrays, respectively. The transmit array elements radiate a narrowband signal centered around the frequency $f$.

Assume the observation model in (2), with the channel matrix given by $\mathbf{H}(\boldsymbol{\theta}_k) \triangleq \alpha_k\mathbf{a}_R(z_k,r_k)\mathbf{a}_T^T(z_k,r_k)$. The transmit and receive steering vectors are given by (see e.g. [49]) $\mathbf{a}_T(z_k,r_k)=e^{j\pi/4}\sqrt{N_T}(\mathbf{T}_T\mathbf{q}(z_k,r_k)/\|\mathbf{T}_T\mathbf{q}(z_k,r_k)\|)$ and $\mathbf{a}_R(z_k,r_k)=e^{j\pi/4}\sqrt{N_R}(\mathbf{T}_R\mathbf{q}(z_k,r_k)/\|\mathbf{T}_R\mathbf{q}(z_k,r_k)\|)$, respectively. The elements of the matrices $\mathbf{T}_T\in\mathbb{C}^{N_T\times M}$ and $\mathbf{T}_R\in\mathbb{C}^{N_R\times M}$ are given by $[\mathbf{T}_T]_{im}=\phi_m(z_{T_i})$ and $[\mathbf{T}_R]_{im}=\phi_m(z_{R_i})$, respectively, where $\phi_m(\cdot)$ is the $m$th modal depth eigenfunction and $M$ denotes the number of propagating modes. The $m$th element of $\mathbf{q}(z_k,r_k)\in\mathbb{C}^{M\times 1}$ is given by $[\mathbf{q}(z_k,r_k)]_m=\phi_m(z_k)(e^{j\kappa_m r_k}/\sqrt{\kappa_m r_k})$, where $\kappa_m$ is the horizontal wavenumber of mode $m$.

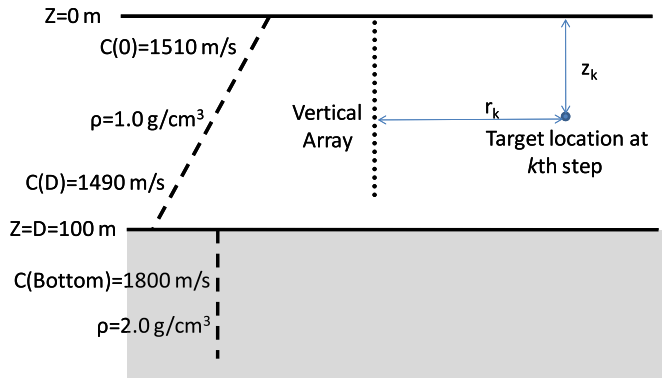


Fig. 3. The Pekeris waveguide with pressure-release surface and penetrable fluid bottom.

Denote the target unknown random parameter vector at the $k$th step by $\boldsymbol{\theta}_{tgt_k}\triangleq[\mathrm{Re}(\alpha_k),\mathrm{Im}(\alpha_k),z_k,r_k,\dot{z}_k,\dot{r}_k]^T$, where the pair $[\dot{z}_k,\dot{r}_k]$ denotes the target velocity along the depth axis and range axis, respectively. Environmental parameters in an underwater waveguide may consist of the sound velocity $c(z)$, the locations of the elements of transmit and receive arrays $\{z_{T_i}\}_{i=1}^{N_T}$ and $\{z_{R_i}\}_{i=1}^{N_R}$, the channel depth $D$, and other possible parameters. It is implicit that $\mathbf{T}_T$, $\mathbf{T}_R$, and $\mathbf{q}$ are dependent of the environmental parameters, where $\mathbf{q}$ depends also on the target location parameters. In the simulations, we assumed that the unknown environmental parameters consist of the channel depth $D_k$, i.e. $\boldsymbol{\theta}_{env_k}=D_k$. The entire unknown vector parameter at the $k$th step is $\boldsymbol{\theta}_k=[\mathrm{Re}(\alpha_k),\mathrm{Im}(\alpha_k),z_k,r_k,\dot{z}_k,\dot{r}_k,D_k]^T$. The optimal transmit signal autocorrelation matrix $\mathbf{R}_{\mathbf{s}_k}^{(opt)}$ is obtained by solving the SDP problem in (10) in which we set the weighting matrix as $\mathbf{W}=\mathrm{diag}(0,0,1,1,0,0,0)$ in order to optimize the performance of target location estimation.

Assume a constant linear state model in (2), where the transition matrix $\mathbf{F}_k$ contains the motion model, which is defined by the commonly used white noise acceleration model [50]. The transition matrix $\mathbf{F}_k$ and state noise covariance $\mathbf{R}_\mathbf{u}$ are given by

$$\mathbf{F}_k=\begin{bmatrix}0.99&0&0&0&0&0&0\\0&0.99&0&0&0&0&0\\0&0&1&0&T&0&0\\0&0&0&1&0&T&0\\0&0&0&0&1&0&0\\0&0&0&0&0&1&0\\0&0&0&0&0&0&1\end{bmatrix} \tag{11}$$

$$\mathbf{R}_\mathbf{u}=\begin{bmatrix}\frac{\sigma_\alpha^2}{2}&0&0&0&0&0&0\\0&\frac{\sigma_\alpha^2}{2}&0&0&0&0&0\\0&0&\delta\frac{T^3}{3}&0&\delta\frac{T^2}{2}&0&0\\0&0&0&\delta\frac{T^3}{3}&0&\delta\frac{T^2}{2}&0\\0&0&\delta\frac{T^2}{2}&0&\delta T&0&0\\0&0&0&\delta\frac{T^2}{2}&0&\delta T&0\\0&0&0&0&0&0&\sigma_D^2\end{bmatrix} \tag{12}$$

where $T>0$ is the time interval between steps and $\delta>0$ indicates the motion process noise intensity. The term $\sigma_\alpha^2$ represents the process noise variance of the target complex attenuation factor. The term $\sigma_D^2$ denotes the process noise variance

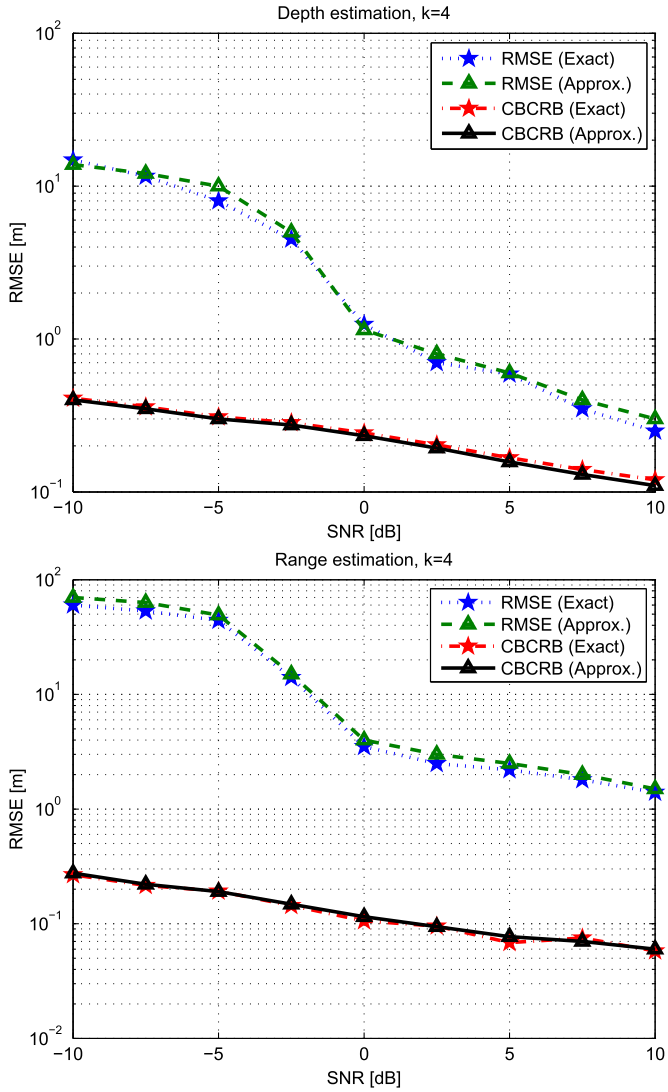


Fig. 4. Comparison between adaptive optimization of exact sequential CBCRB criterion and the approximate sequential CBCRB criterion, vs. SNR. Depth estimation performance and CBCRB (top) and range estimation performance and CBCRB (bottom). The values were calculated at the 4th step.

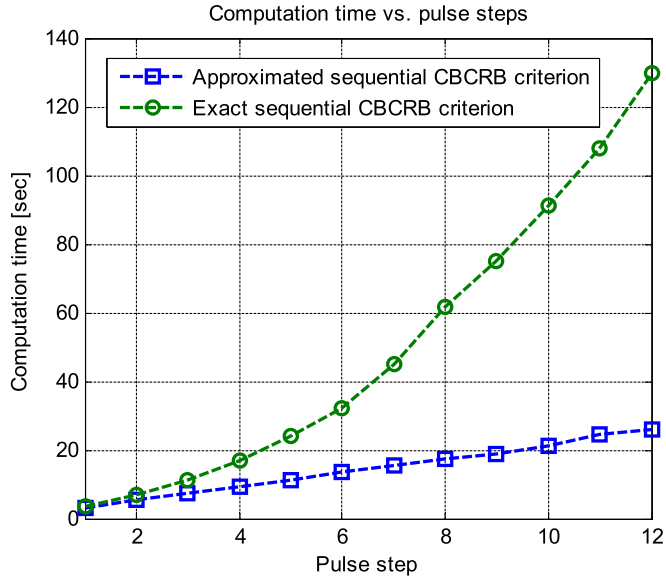


Fig. 5. Computation time versus pulse steps using the exact sequential CBCRB and its approximation as optimization criteria.

of the channel depth. In the simulations, we used $T = 2$ sec, $\delta = 0.1$ m$^2$/sec$^3$, $\sigma_\alpha^2 = 0.02$, and $\sigma_D^2 = 0.01$ m$^2$.

Consider the observation model as in (2), where the additive Gaussian noise matrix $\mathbf{N}_k$ is randomly generated at each step of each trial. We assume spatially white noise at the receive array elements, $\mathbf{R} = \sigma^2\mathbf{I}_N$. The total SNR at time step $k = 0$ is defined as $SNR \triangleq P\mathrm{E}\big[|\alpha_0|^2\big]\|\mathbf{a}_T(z_0, r_0, D_0)\|^2\|\mathbf{a}_R(z_0, r_0, D_0)\|^2/\sigma^2 N_T N_R$. Since $\mathbf{a}_T$ and $\mathbf{a}_R$ are normalized steering vectors, the total SNR at time step $k = 0$ becomes $SNR \triangleq P(\mathrm{E}[|\alpha_0|^2]/\sigma^2)$.

Consider the following definition of the 2-dimensional transmit beampattern, which describes the transmitted energy distribution over the $[z, r]$ plane calculated for the true channel depth $D_k$ at the $k$th step:

$$Q(z, r) \triangleq \mathbf{a}_T^H(z, r, D_k)\mathbf{R}_{\mathbf{s}_k}^* \mathbf{a}_T(z, r, D_k) \qquad (13)$$

In the following scenarios, the number of propagating modes, $M$, remains constant for all cases of channel depth uncertainty. The target tracking performance is evaluated in terms of the RMSE of the MMSE estimator of the state vector $\boldsymbol{\theta}_k$ at the $k$th step, given by $\hat{\boldsymbol{\theta}}_k(\mathbf{X}^{(k)}) = \mathrm{E}[\boldsymbol{\theta}_k|\mathbf{X}^{(k)}]$.

The sound speed varies from $c(0) = 1510$ m/s at the surface, and $c(D_0) = 1490$ m/s at the bottom. The sound speed at the sediment depths is $C(Bottom) = 1800$ m/s. The initial waveguide depth is $D_0 = 100$ m. We use a vertical uniform linear array (ULA) of $N_T = N_R = N = 9$ transceivers. The elements of the arrays are equally spaced along the channel depth and the inter-element spacing is $1.11\lambda_{min}$, where $\lambda_{min}$ is the minimal wavelength in the waveguide given by $\lambda_{min} = c(D_0)/f$. The transmit array radiates a narrowband signal centered at frequency $f = 150$ Hz. The $m$th modal eigenfunction $\phi_m(\cdot)$ and the $m$th vertical and horizontal wavenumbers, given by $\gamma_m$ and $\kappa_m$, respectively, were computed using numerical simulations based on the KRAKEN normal mode program [53]. This constellation supports $M = 11$ propagating modes. Higher order modes penetrate the bottom halfspace and do not propagate in the waveguide.

Assume uniform prior distribution for the unknown target dynamics parameters as $\alpha_0 \sim CN(0, 10)$, $z_0 \sim U[0, 100$ m$]$, $r_0 \sim U[1000$ m$, 1350$ m$]$, $\dot{z}_0 \sim U[-2$ m/sec$, 2$ m/sec$]$, $\dot{r}_0 \sim U[-10$ m/sec$, 10$ m/sec$]$. The unknown environmental parameter is the channel depth $D_k$, which is initially uniformly distributed $D_0 \sim U[100$ m $- \triangle/2, 100$ m $+ \triangle/2]$, where $\triangle$ represents the uncertainty of the channel depth. The number of snapshots in each pulse step is $L = 9$. The simulations were performed for 500 trials. The initial value of the state vector was determined as $[\mathrm{Re}(\alpha_0), \mathrm{Im}(\alpha_0), z_0, r_0, \dot{z}_0, \dot{r}_0, D_0] = [0, 1, 75$ m$, 1250$ m$, -1$ m/sec$, -5$ m/ses$, 100$ m$]$ and the channel depth uncertainty as $\triangle = 0.1$ m.

Fig. 4 compares the performances of the exact sequential CBCRB and the approximate sequential CBCRB, in terms of range and depth estimation performance vs. SNR. The transmit beampatterns were optimized according to the SDP problem in (10). The upper curves represent the average squared root MSE (RMSE) of the target location MMSE estimation, for two optimization criteria, given by the exact sequential CBCRB and its approximation. The location MMSE estimator is obtained via

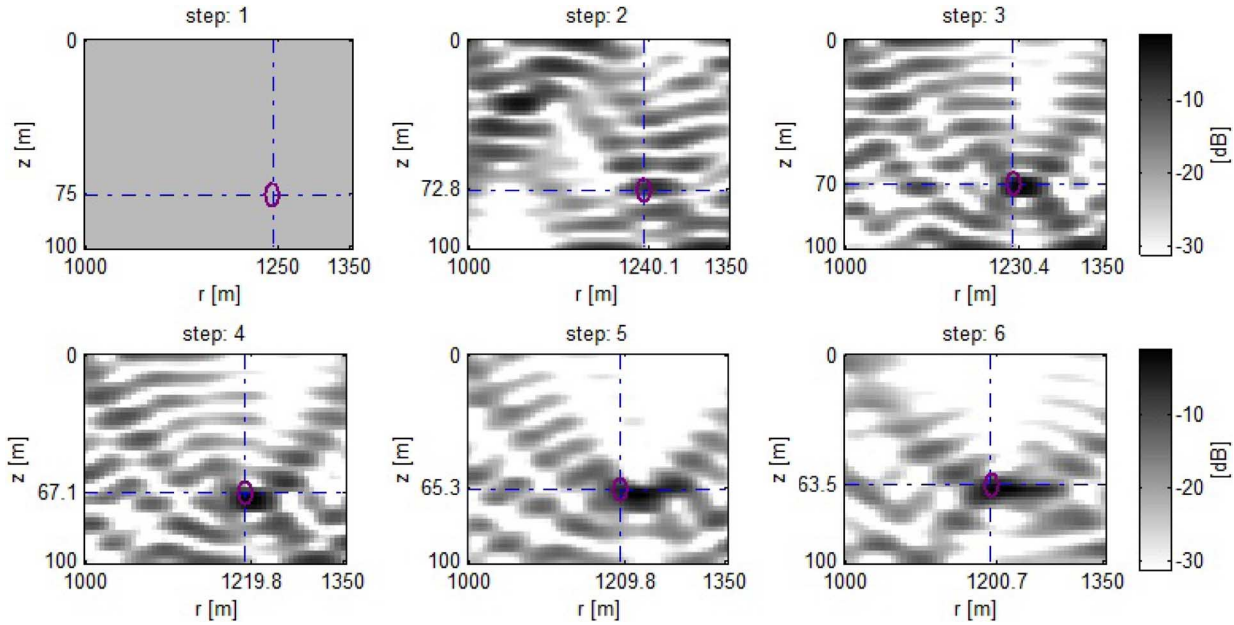


Fig. 6. Optimal transmit beampatterns vs. pulse step, $SNR = 0$ dB. The circle represents the target location vector at the $k$th step $[z_k, r_k]^T$.

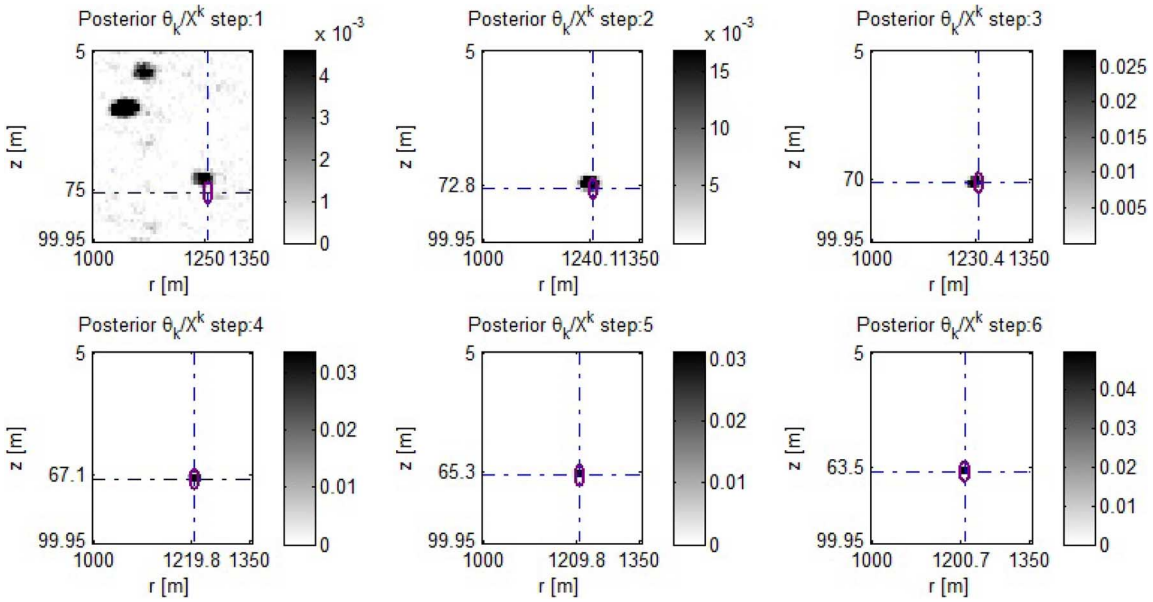


Fig. 7. State *posterior* pdf vs. pulse steps, $SNR = 0$ dB. The circle represents the target location vector at the $k$th step $[z_k, r_k]^T$.

the state posterior pdf $f_{\boldsymbol{\theta}_k|\mathbf{X}^{(k)}}$, which is available at the end of $k$th step. The lower curves represent the sequential CBCRB and its approximation. It can be seen that the performance difference between the two criteria is almost indistinguishable.

Fig. 5 compares the computation time between the sequential CBCRB and its approximation based transmit beamforming vs. the pulse steps. The processing time is obtained by running the adaptive algorithms using Matlab on a 2.4 GHz Intel core i7 4500U processor and memory of 4 GB 1600 MHz DDR3. The computation time was averaged over 500 trials under the scenario considered above. The number of particles in each trial is $N_s = 7000$. It can be seen that the computational complexity of the transmit beamforming technique based on the exact sequential CBCRB criterion is higher compared to the approximate sequential CBCRB criterion, which is consistent with the computational complexity analysis performed in Section IV-B. Consequently, all the simulations which follow were performed w.r.t. the approximate sequential CBCRB as an optimization criterion.

Figs. 6 and 7 show the evolution of the transmit beampattern and state posterior pdf vs. the pulse steps, respectively. The simulation was performed for $SNR = 0$ dB. The beampatterns were calculated according to (13). The first transmit beampattern is omnidirectional, corresponding to the initial uncertainty of the target position. It can be seen that the simulated scenario produces high sidelobes, due to the spatial undersampling of the channel depth. The adaptive algorithm converges to the true position of the target at pulse step $k = 3$, in which the beampattern focuses on the target position.

The proposed adaptive transmit beamforming is compared to the following beamforming methods; (1) orthogonal waveforms are transmitted via each element, i.e.

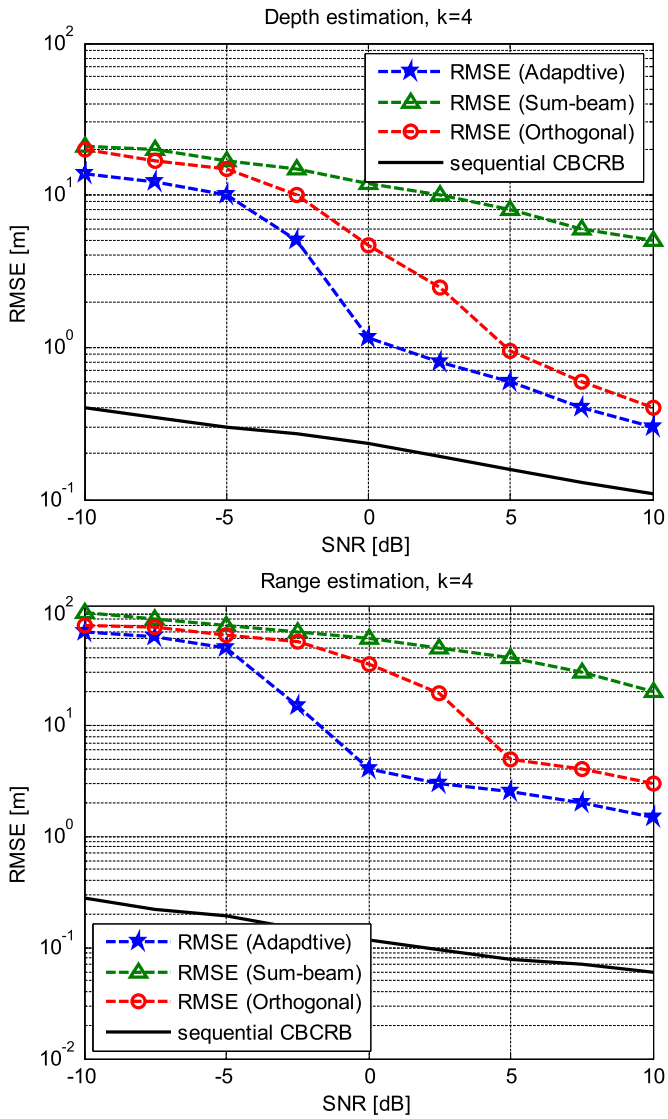


Fig. 8. RMSE for estimation of target depth (top) and range (bottom), a comparison adaptive beamforming, sum-beam beamforming and orthogonal beamforming, for channel depth uncertainty $\triangle = 0.1$ m. The bottom curve represents the CBCRB for parameter estimation. The upper curves represent the parameter estimation performance in terms of RMSE, for each transmit beamforming technique. The values were calculated at the 4th step.

$\mathbf{R}_{\mathbf{s}_k} = (P/N_T)\mathbf{I}_{N_T}$, (2) transmitting sum-beam steered towards the predicted MMSE estimate of the target location, i.e. $\mathbf{R}_{\mathbf{s}_k} = (P/N_T)\mathbf{a}_T^*(\hat{\boldsymbol{\varphi}}_{k/k-1})\mathbf{a}_T^T(\hat{\boldsymbol{\varphi}}_{k/k-1})$, where $\hat{\boldsymbol{\varphi}}_{k/k-1} = \mathrm{E}[\boldsymbol{\varphi}_k|\mathbf{X}^{(k-1)}]$ and the expectation is performed w.r.t. the state prediction pdf $f_{\boldsymbol{\varphi}_k|\mathbf{X}^{(k-1)}}$ using MC integration. For each method the conditional mean estimator for target location estimation was implemented. It is obtained via the state posterior pdf $f_{\boldsymbol{\theta}_k|\mathbf{X}^{(k)}}$, which is available at the end of $k$th step. In Fig. 8 we compare the RMSE obtained using the proposed adaptive beamforming to fixed orthogonal beamforming and to the predicted MMSE sum-beam, for several SNR's. The RMSE's were calculated at the 4th step. It is evident that the adaptive beamforming for a dynamic target performs better than fixed beamforming and sum-beam methods. The asymptotic difference between the RMSE performance of the adaptive beamforming and the sequential CBCRB is due to the fact that the BCRB is not guaranteed to be achieved even asymptotically (see e.g. [54]).

## VI. Conclusion

In this paper, we presented a new cognitive beamforming method for target tracking in the presence of model uncertainties. The CBCRB on the prediction error of the parameters of interest in the state-vector was used as the optimization criterion for beampattern design at each step. A recursive method for computing the CBCRB was derived. A low-complexity method for computing an approximation of the CBCRB was proposed. The proposed method was tested via simulations for the problem of target tracking in a shallow underwater environment. The results show that even at very low SNR's, the proposed method automatically focuses the transmit beampattern toward the predicted target location. The performance of the proposed method was compared to other methods, such as invariant, omni-directional transmission, and it was shown that the proposed method has superior performance.

Future research can focus on the analysis of high sidelobe environments, where the beampattern optimization needs to be performed using large-error bounds.

## Appendix
## Derivation of the Sequential Conditional BCRB in (3)

In this appendix, it is shown that the sequential CBCRB for estimating $\boldsymbol{\theta}_k$, as presented in Section III-A, using the state and observation models in (2), is given by (3).

The sequential CBCRB sets a bound on the MSE of estimating the state vector $\boldsymbol{\theta}_k$ from new observation $\mathbf{X}_k$ given a random matrix $\mathbf{Y}$, which may consist of several random vectors. Denote $\hat{\boldsymbol{\theta}}^{(k)}(\mathbf{Y})$ as the estimate of $\boldsymbol{\theta}^{(k)}$, dependent of a random matrix $\mathbf{Y}$. Then, the MSE matrix of the estimate for $\boldsymbol{\theta}^{(k)}$, is bounded by [38]

$$\mathrm{E}\left[\left(\hat{\boldsymbol{\theta}}^{(k)}(\mathbf{Y})-\boldsymbol{\theta}^{(k)}\right)\left(\hat{\boldsymbol{\theta}}^{(k)}(\mathbf{Y})-\boldsymbol{\theta}^{(k)}\right)^T\middle|\mathbf{Y}\right] \succeq \mathbf{C}_{\boldsymbol{\theta}^{(k)}}(\mathbf{Y}) = \mathbf{J}^{-1}_{\boldsymbol{\theta}^{(k)}}(\mathbf{Y}) \quad (14)$$

where $\mathbf{C}_{\boldsymbol{\theta}^{(k)}}(\mathbf{Y})$ and $\mathbf{J}^{-1}_{\boldsymbol{\theta}^{(k)}}(\mathbf{Y})$ are the conditional BCRB and BFIM for estimating $\boldsymbol{\theta}^{(k)}$ from new observation $\mathbf{X}_k$ given a random matrix $\mathbf{Y}$, respectively. Define $\mathbf{C}_{\boldsymbol{\theta}_k}(\mathbf{Y})$ as the CBCRB for estimating $\boldsymbol{\theta}_k$, derived from the lower right submatrix of $\mathbf{C}_{\boldsymbol{\theta}^{(k)}}(\mathbf{Y})$. Define the corresponding equivalent BFIM as $\mathbf{J}_{\boldsymbol{\theta}_k}(\mathbf{Y}) = \mathbf{C}^{-1}_{\boldsymbol{\theta}_k}(\mathbf{Y})$. In [38] it was shown that $\mathbf{J}_{\boldsymbol{\theta}_k}(\mathbf{Y})$ can be calculated sequentially as follows

$$\mathbf{J}_{\boldsymbol{\theta}_k}(\mathbf{Y}) = \mathbf{D}_k^{22}(\mathbf{Y}) - \mathbf{D}_k^{21}(\mathbf{Y})\left(\mathbf{J}_{\boldsymbol{\theta}_{k-1}}(\mathbf{Y})+\mathbf{D}_k^{11}(\mathbf{Y})\right)^{-1}\mathbf{D}_k^{12}(\mathbf{Y}) \quad (15)$$

where

$$\mathbf{D}_k^{11}(\mathbf{Y}) = \mathrm{E}\left[-\frac{\partial^2 \log f_{\boldsymbol{\theta}_k|\boldsymbol{\theta}_{k-1}}}{\partial \boldsymbol{\theta}_{k-1}^2}\middle|\mathbf{Y}\right] \quad (16)$$

$$\mathbf{D}_k^{12}(\mathbf{Y}) = \mathrm{E}\left[-\frac{\partial^2 \log f_{\boldsymbol{\theta}_k|\boldsymbol{\theta}_{k-1}}}{\partial \boldsymbol{\theta}_k \partial \boldsymbol{\theta}_{k-1}}\middle|\mathbf{Y}\right] = \left(\mathbf{D}_k^{21}(\mathbf{Y})\right)^T \quad (17)$$

$$\mathbf{D}_k^{22}(\mathbf{Y}) = \mathrm{E}\left[ -\frac{\partial^2 \log f_{\boldsymbol{\theta}_k|\boldsymbol{\theta}_{k-1}}}{\partial \boldsymbol{\theta}_k^2} - \frac{\partial^2 \log f_{\mathbf{x}_k|\boldsymbol{\theta}_k}}{\partial \boldsymbol{\theta}_k^2} \middle| \mathbf{Y} \right]. \tag{18}$$

Proof of (15) is given in [38].

The state model presented in (2) is linear with additive i.i.d zero-mean real Gaussian noise process with a covariance matrix $\mathbf{R_u}$. Therefore, the density function of the state vector at the $k$th step is Gaussian given the $(k-1)$th state vector, i.e. $\boldsymbol{\theta}_k|\boldsymbol{\theta}_{k-1} \sim N(\mathbf{F}_k\boldsymbol{\theta}_{k-1}, \mathbf{R}_u)$. From this assumption, it follows that

$$\log f_{\boldsymbol{\theta}_k|\boldsymbol{\theta}_{k-1}} = \tilde{c} - \frac{1}{2}\left(\boldsymbol{\theta}_k - \mathbf{F}_k\boldsymbol{\theta}_{k-1}\right)^T \mathbf{R}_u^{-1}\left(\boldsymbol{\theta}_k - \mathbf{F}_k\boldsymbol{\theta}_{k-1}\right) \tag{19}$$

where $\tilde{c}$ is a constant. Substituting (19) into (16)–(18) yields

$$\mathbf{D}_k^{11}(\mathbf{Y}) = \mathbf{F}_k^T\mathbf{R}_{\mathbf{u}}^{-1}\mathbf{F}_k \tag{20}$$

$$\mathbf{D}_k^{12}(\mathbf{Y}) = -\mathbf{F}_k^T\mathbf{R}_{\mathbf{u}}^{-1} = \left(\mathbf{D}_k^{21}(\mathbf{Y})\right)^T \tag{21}$$

$$\mathbf{D}_k^{22}(\mathbf{Y}) = \mathbf{R}_{\mathbf{u}}^{-1} - \mathrm{E}\left[ \frac{\partial^2 \log f_{\mathbf{x}_k|\boldsymbol{\theta}_k}}{\partial \boldsymbol{\theta}_k^2} \middle| \mathbf{Y} \right]. \tag{22}$$

According to (2), the conditional density function of the state vector at the $k$th step is complex Gaussian given the $k$th state vector, i.e. $\boldsymbol{X}_k|\boldsymbol{\theta}_k \sim CN(\mathbf{H}(\boldsymbol{\theta}_k)\mathbf{S}_k, \mathbf{R})$. Define the second part of (22) as the incremental CBFIM for estimating $\boldsymbol{\theta}_k$ from $\mathbf{X}_k$, conditioned on a random matrix $\mathbf{Y}$, given by $\triangle\mathbf{J}_{\boldsymbol{\theta}_k}(\mathbf{Y}) \triangleq -\mathrm{E}[(\partial^2 \log f_{\mathbf{X}_k|\boldsymbol{\theta}_k}/\partial\boldsymbol{\theta}_k^2)|\mathbf{Y}]$. In [17] it was shown that $\triangle\mathbf{J}_{\boldsymbol{\theta}_k}(\mathbf{Y})$ is given by

$$\triangle\mathbf{J}_{\boldsymbol{\theta}_k}(\mathbf{Y}) = 2L\mathrm{Re}\left\{\mathbf{V}_{N_\theta}\left[\boldsymbol{\Gamma}_{\boldsymbol{\theta}_k}(\mathbf{Y}) \odot \left[\mathbf{1}_{N_\theta\times N_\theta} \otimes \mathbf{R}_{\mathbf{s}_k}^T\right]\right]\mathbf{V}_{N_\theta}^T\right\} \tag{23}$$

where $\mathbf{R}_{\mathbf{s}_k} \triangleq (1/L)\mathbf{S}_k\mathbf{S}_k^H$ denotes the $k$th transmit autocorrelation matrix, and $\boldsymbol{\Gamma}_{\boldsymbol{\theta}_k}(\mathbf{Y})$ is given by

$$\boldsymbol{\Gamma}_{\boldsymbol{\theta}_k}(\mathbf{Y}) \triangleq \mathrm{E}\left[ \dot{\mathbf{H}}^H(\boldsymbol{\theta}_k)\mathbf{R}^{-1}\dot{\mathbf{H}}(\boldsymbol{\theta}_k) \middle| \mathbf{Y} \right] \tag{24}$$

where the expectation in (24) at the $k$th step is performed w.r.t. the conditional pdf $f_{\boldsymbol{\theta}_k|\mathbf{Y}}$. Inserting the incremental CBFIM in (23) into the second part of (22) and replacing the conditioning on the random matrix $\mathbf{Y}$ in (20)–(22), and (24) with the history observations $\mathbf{X}^{(k-1)}$, yields the recursive relation in (3).

## REFERENCES


[1] I. Bekkerman and J. Tabrikian, "Spatially coded signal model for active arrays," in *Proc. ICASSP*, May 2004, vol. 2, pp. 209–212.

[2] I. Bekkerman and J. Tabrikian, "Target detection and localization using MIMO radars and sonars," *IEEE Trans. Signal Process.*, vol. 54, no. 10, pp. 3873–3883, Oct. 2006.

[3] E. Fishler, A. Haimovich, R. S. Blum, D. Chizhik, L. J. Cimini, and R. A. Valenzuela, "Spatial diversity in radars-models and detection performance," *IEEE Trans. Signal Process.*, vol. 54, no. 3, pp. 823–838, Mar. 2006.

[4] L. Xu, J. Li, and P. Stoica, "Target detection and parameter estimation for MIMO radar systems," *IEEE Trans. Aerosp. Electron. Syst.*, vol. 44, no. 7, pp. 927–939, Jul. 2008.

[5] H. Deng and B. Himed, "A virtual antenna beamforming (VAB) approach for radar systems by using orthogonal coding waveforms," *IEEE Trans. Antennas Propag.*, vol. 57, no. 2, pp. 425–435, Feb. 2009.

[6] J. Li and P. Stoica, *MIMO Radar Signal Process*. Hoboken, NJ, USA: Wiley, 2009.

[7] W. Roberts, P. Stoica, J. Li, T. Yardibi, and F. A. Sadjadi, "Iterative adaptive approaches to MIMO radar imaging," *IEEE J. Selected Topics in Signal Processing*, vol. 4, no. 1, pp. 5–20, Feb. 2010.

[8] J. Tabrikian, "Barankin bounds for target localization by MIMO radars," in *Proc. IEEE Workshop Sens. Array Multichannel Process.*, Jul. 2006, pp. 287–281.

[9] R. Niu, R. S. Blum, P. K. Varshney, and A. L. Drozd, "Target localization and tracking in noncoherent MIMO radar systems," *IEEE Trans. Aerosp. Electron. Syst.*, vol. 48, no. 2, pp. 1466–1489, Apr. 2012.

[10] J. Li, L. Xu, P. Stoica, K. W. Forsythe, and D. W. Bliss, "Range compression and waveform optimization for MIMO radar: A Cramér-Rao bound based study," *IEEE Trans. Signal Process.*, vol. 56, no. 1, pp. 218–232, Jan. 2008.

[11] P. Stoica, J. Li, and X. Zhu, "Waveform synthesis for diversity-based transmit beampattern design," *IEEE Trans. Signal Process.*, vol. 56, no. 6, pp. 2593–2598, Jun. 2008.

[12] P. Stoica, J. Li, and Y. Xie, "On probing signal design for MIMO radar," *IEEE Trans. Signal Process.*, vol. 55, no. 8, pp. 4151–4161, Aug. 2007.

[13] S. Ahmed, J. S. Thompson, Y. R. Petillot, and B. Mulgrew, "Unconstrained synthesis of covariance matrix for MIMO radar transmit beampattern," *IEEE Trans. Signal Process.*, vol. 59, no. 8, pp. 3837–3849, May 2011.

[14] B. Yazici and G. Xie, "Wideband extended range-Doppler imaging and waveform design in the presence of clutter and noise," *IEEE Trans. Inf. Theory*, vol. 52, no. 10, pp. 4563–4580, Oct. 2006.

[15] E. Grossi and M. Lops, "Space-time code design for MIMO detection based on Kullbak-Leibler divergence," *IEEE Trans. Inf. Theory*, vol. 58, no. 6, pp. 3989–4004, Jun. 2012.

[16] J. Yuanwei, J. Moura, and N. O'Donoughue, "Time-Reversal in Multiple-Input Multiple-Output Radar," *IEEE Trans. Signal Process.*, vol. 4, no. 1, pp. 210–225, Feb. 2010.

[17] W. Huleihel, J. Tabrikian, and R. Shavit, "Optimal adaptive waveform design for cognitive MIMO radar," *IEEE Trans. Signal Process.*, vol. 61, no. 20, pp. 5075–5089, Oct. 2013.

[18] A. Leshem, O. Naparstek, and A. Nehorai, "Information theoretic adaptive radar waveform design for multiple extended targets," *IEEE J. Sel. Topics Signal Process.*, vol. 1, no. 1, pp. 42–55, Jun. 2007.

[19] J. Tabrikian, "Adaptive waveform design for target enumeration in cognitive radar," in *Proc. IEEE 5th Int. Workshop Comput. Adv. Multi-Sensor Adaptive Process. (CAMSAP)*, Dec. 2013, pp. 69–72.

[20] I. Reuven and H. Messer, "A Barankin-type lower bound on the estimation error of a hybrid parameter vector," *IEEE Trans. Inf. Theory*, vol. 43, no. 3, pp. 1084–1093, May 1997.

[21] M. Hurtado, T. Zhao, and A. Nehorai, "Adaptive polarized waveform design for target tracking based on sequential Bayesian inference," *IEEE Trans. Signal Process.*, vol. 56, no. 3, pp. 1120–1133, Mar. 2008.

[22] S. P. Sira, Y. Li, A. Papandreou-Suppappola, D. Morrell, D. Cochran, and M. Rangaswamy, "Waveform-agile sensing for tracking," *IEEE Signal Process. Mag.*, vol. 26, no. 1, pp. 53–64, Jan. 2009.

[23] S. Sen and A. Nehorai, "OFDM MIMO radar with mutual-information waveform design for low-grazing angle tracking," *IEEE Trans. Signal Process.*, vol. 58, no. 6, pp. 3152–3162, Jun. 2010.

[24] D. J. Kershaw and R. J. Evans, "Optimal waveform selection for tracking systems," *IEEE Trans. Inf. Theory*, vol. 40, no. 5, pp. 1536–1550, Sep. 1994.

[25] D. J. Kershaw and R. J. Evans, "Waveform selective probabilistic data association," *IEEE Trans. Aerosp. Electron. Syst.*, vol. 33, no. 4, pp. 1180–1188, Oct. 1997.

[26] S. Suvorova, D. Musicki, B. Moran, S. Howard, and B. La Scala, "Multi-step ahead beam and waveform scheduling for tracking of maneuvering targets in clutter," in *Proc. IEEE Int. Conf. Acoust., Speech, Signal Process.*, Philadelphia, PA, USA, Mar. 2005, pp. 889–892.

[27] S. P. Sira, A. Papanderou-Suppappola, D. Morrell, and D. Cochran, "Waveform-agile sensing for tracking multiple targets in clutter," in *Proc. Conf. Inf. Sci. Syst. Special Session Waveform Adaptive Sens.*, Princeton, NJ, USA, Mar. 2006, pp. 1418–1423.

[28] M. Simandl, J. Kralovec, and P. Tichavsky, "Filtering, predictive, smoothing Cramér-Rao bounds for discrete-time nonlinear dynamic systems," *Automatica*, vol. 37, pp. 1703–1716, Apr. 2001.

[29] P. Stano, Z. Lendek, J. Braaksma, R. Babuska, C. de Keizer, and A. J. den Dekker, "Parametric Bayesian filters for nonlinear stochastic dynamical systems: A survey," *IEEE Trans. Cybern.*, vol. 43, no. 6, pp. 1607–1624, Dec. 2013.

[30] F. Gustafsson, "Particle filter theory and practice with positioning applications," *IEEE Aerosp. Elec. Syst. Mag.*, vol. 25, no. 7, pp. 53–83, Jul. 2010.

[31] R. Karlsson and N. Bergman, "Auxiliary particle filters for tracking a maneuvering target," in *Proc. IEEE 39th Conf. Decision Control*, Dec. 2000, vol. 4, pp. 3891–3895.

[32] M. K. Pitt and N. Shephard, "Filtering via simulation: Auxiliary particle filters," *J. Amer. Statist. Assoc.*, vol. 94, no. 446, pp. 590–599, Jun. 1999.
[33] M. S. Arulampalam, S. Maskell, N. Gordon, and T. Clapp, "A tutorial on particle filters for online nonlinear/non-Gaussian Bayesian tracking," *IEEE Trans. Signal Process.*, vol. 50, no. 2, pp. 174–188, Feb. 2002.
[34] N. J. Gordon, D. J. Salmond, and A. F. M. Smith, "Novel approach to nonlinear/non-Gaussian Bayseian state estimation," *Proc. IEEE*, vol. 140, pp. 107–113, Apr. 1993.
[35] M. Zoubir and D. R. Iskander, "The bootstrap: A tutorial for the signal processing practitioner," *IEEE Signal Process. Mag.*, vol. 24, no. 4, pp. 10–19, Jul. 2007.
[36] J. Tabrikian and J. L. Krolik, "Efficient computation of the Bayesian Cramér-Rao bound on estimating parameters of Markov models," in *Proc. IEEE Int. Conf. Acoust., Speech, Signal Process.*, Mar. 1999, vol. 3, pp. 1761–1764.
[37] P. Tichavsky, C. H. Muravchik, and A. Nehorai, "Posterior Cramér-Rao bounds for discrete-time nonlinear filtering," *IEEE Trans. Signal Process.*, vol. 46, no. 5, pp. 1386–1396, May 1998.
[38] L. Zuo, R. Niu, and P. K. Varshney, "Conditional posterior Cramér-Rao Lower bounds for nonlinear sequential Bayesian estimation," *IEEE Trans. Signal Process.*, vol. 59, no. 1, pp. 1–14, Jan. 2011.
[39] J. Tabrikian and H. Messer, "Three-dimensional source localization in a waveguide," *IEEE Trans. Signal Process.*, vol. 44, no. 1, pp. 1–13, Jun. 1996.
[40] A. Jakoby, J. Goldberg, and H. Messer, "Source localization in shallow water in the presence of sensor location uncertainty," *IEEE J. Ocean. Eng.*, vol. 25, no. 3, pp. 331–336, Jul. 2000.
[41] W. Xu, A. B. Baggeroer, and H. Schmidt, "Performance analysis for matched-field source localization: Simulations and experimental results," *IEEE J. Ocean. Eng.*, vol. 31, no. 2, pp. 325–344, Apr. 2006.
[42] W. Xu, A. B. Baggeroer, and C. D. Richmond, "Bayesian bounds for matched-field parameter estimation," *IEEE Trans. Signal Process.*, vol. 52, no. 12, pp. 3293–3305, Dec. 2004.
[43] J. Tabrikian, G. S. Fostick, and H. Messer, "Detection of environmental mismatch in a shallow water waveguide," *IEEE Trans. Signal Process.*, vol. 47, no. 8, pp. 2181–2190, Aug. 1999.
[44] J. Tabrikian, J. L. Krolik, and H. Messer, "Robust maximum likelihood source localization by exploiting predictable acoustic modes," in *Proc. ICASSP*, 1996, vol. 6, pp. 3089–3092.
[45] S. Narasimhan and J. L. Krolik, "A Cramér-Rao bound for source range estimation in a random ocean waveguide," in *Proc. IEEE Workshop Statist. Signal Array Process.*, 1994, pp. 309–312.
[46] S. Boyd and L. Vandenberghe, *Convex Optimization*. New York, NY, USA: Cambridge Univ. Press, 2004.
[47] L. Vandenberghe and S. Boyd, "Semidefinite Programming," *SIAM Rev.*, vol. 38, no. 1, pp. 49–95, Mar. 1996.
[48] L. Vandenberghe, S. Boyd, and S. P. Wu, "Determinant maximization with linear matrix inequality constraints," *SIAM J. Matrix Anal. Applicat.*, vol. 19, no. 2, pp. 499–533, Apr. 1998.
[49] I. Tolstoy and C. S. Clay, *Ocean Acoustics*. New York, NY, USA: McGraw-Hill, 1966.
[50] Y. Bar-Shalom, X. R. Li, and T. Kirubarajan, *Estimation with Applications to Tracking and Navigation*. New York, NY, USA: Wiley, 2001.
[51] H. Li, "Complex-valued adaptive signal processing using Wirtinger calculus and its application to independent component analysis," Ph.D. dissertation, Univ. of Maryland Baltimore County, Baltimore, MD, USA, 2008.
[52] J. Löfberg, "YALMIP: A toolbox for modeling and optimization in MATLAB," in *Proc. CACSD Conf.*, Taipei, Taiwan, 2004.
[53] M. B. Porter, The KRAKEN Normal Mode Program. Naval Res. Lab., Washington, DC, 1992.
[54] H. L. Van Trees and K. L. Bell, *Bayesian Bounds for Parameter Estimation and Nonlinear Filtering/Tracking*. New York, NY, USA: Wiley, 2007.
[55] F. B. Jensen, W. A. Kuperman, M. B. Porter, and H. Schmidt, *Computational Ocean Acoustics*, 2nd ed. New York, NY, USA: Springer, 2011.

**Nathan Sharaga** was born in Israel, 1986. He received the B.Sc. in electrical engineering from the Technion Institute of Technology, Haifa, Israel, in 2009 and the M.Sc. in electrical engineering from Tel-Aviv University, Tel-Aviv, Israel, in 2015. From 2009 to 2015, he was an Underwater Systems Engineer for the Israel Navy (IN), and, since 2015, he is a R&D Engineer in Elisra, Israel. His interests include array signal processing, RF signal processing and estimation theory.

**Joseph Tabrikian** (S'89–M'97–SM'98) received the B.Sc., M.Sc., and Ph.D. degrees in electrical engineering from the Tel-Aviv University, Tel-Aviv, Israel, in 1986, 1992, and 1997, respectively. During 1996–1998 he was with the Department of Electrical and Computer Engineering, Duke University, Durham, NC, as an Assistant Research Professor. He is now with the Department of Electrical and Computer Engineering, and Ben-Gurion University of the Negev, Beer-Sheva, Israel. He served as Associate Editor of the IEEE TRANSACTIONS ON SIGNAL PROCESSING during 2001–2004, and 2011–2015 and as Associate Editor of the IEEE SIGNAL PROCESSING LETTERS since 2012–2015. Since 2015 he has been a Senior Area Editor of the IEEE SIGNAL PROCESSING LETTERS. He is a member of the IEEE SAM technical committee since 2010 and was the technical program co-chair of the IEEE SAM 2010 workshop. He is co-author of 5 award-winning papers in different IEEE conferences. His research interests include estimation and detection theory and array signal processing.

**Hagit Messer** (F'00) received the Ph.D. in electrical engineering from Tel-Aviv University (TAU), Israel, and after a post-doctoral fellowship at Yale University, she joined the faculty of Engineering at Tel-Aviv University in 1986, where she is a Professor of Electrical Engineering. In 2000–2003 she has been on leave from TAU, serving as the Chief Scientist at the Ministry of Science. After returning to TAU she was the head of the Porter school of environmental studies (2004–2006), and the Vice President for Research and Development 2006–2008. Then, she has been the President of the Open University, and from Oct. 2013 she serves as the Vice Chair of the Council of Higher Education, Israel. Prof. Messer, Fellow of the IEEE, is an expert in statistical signal processing with applications to source localization, communication and environmental monitoring. She has published numerous journal and conference papers, and has supervised tens of graduate students. She has been a member of Technical committees of the Signal Processing society since 1993 and on the editorial boards of the IEEE TRANSACTIONS ON SIGNAL PROCESSING, the IEEE SIGNAL PROCESSING LETTERS, the IEEE JOURNAL OF SELECTED TOPICS IN SIGNAL PROCESSING (J-STSP), and on the Overview Editorial Board of the Signal Processing Society journals.